Applied Surface Science 393 (2017) 119–126

Contents lists available at ScienceDirect

Applied Surface Science

journal homepage: www.elsevier.com/locate/apsusc

Full Length Article

Germanium nitride and oxynitride films for surface passivation of Ge radiation detectors

G. Maggioni[a,b,*], S. Carturan[a,b], L. Fiorese[b,c], N. Pinto[d,e], F. Caproli[d,e], D.R. Napoli[b], M. Giarola[f], G. Mariotto[f]

[a] Dipartimento di Fisica e Astronomia G. Galilei, Università di Padova, Via Marzolo 8, I-35131 Padova, Italy
[b] Laboratori Nazionali di Legnaro, Istituto Nazionale di Fisica Nucleare, Viale dell'Universita'2, I-35020 Legnaro, Padova, Italy
[c] Dipartimento di Ingegneria dei Materiali e delle Tecnologie Industriali, Università di Trento, Via Mesiano 77, I-38050 Povo, Trento, Italy
[d] Scuola di Scienze e Tecnologie, Sezione di Fisica, Università di Camerino, Via Madonna delle Carceri 9, Camerino, Italy
[e] INFN, Sezione di Perugia, Perugia, Italy
[f] Dipartimento di Informatica—Università di Verona, Strada le Grazie 15, I-37134 Verona, Italy

ARTICLE INFO

Article history:
Received 6 June 2016
Received in revised form 9 September 2016
Accepted 2 October 2016
Available online 4 October 2016

Keywords:
Germanium nitride layer
Germanium oxynitride layer
Room temperature deposition
Electrical resistivity
Surface passivation
Hyperpure germanium detector

ABSTRACT

This work reports a detailed investigation of the properties of germanium nitride and oxynitride films to be applied as passivation layers to Ge radiation detectors. All the samples were deposited at room temperature by reactive RF magnetron sputtering. A strong correlation was found between the deposition parameters, such as deposition rate, substrate bias and atmosphere composition, and the oxygen and nitrogen content in the film matrix. We found that all the films were very poorly crystallized, consisting of very small Ge nitride and oxynitride nanocrystallites, and electrically insulating, with the resistivity changing from three to six orders of magnitude as a function of temperature. A preliminary test of these films as passivation layers was successfully performed by depositing a germanium nitride film on the intrinsic surface of a high-purity germanium (HPGe) diode and measuring the improved performance, in terms of leakage current, with respect to a reference passivated diode. All these interesting results allow us to envisage the application of this coating technology to the surface passivation of germanium-based radiation detectors.

1. Introduction

Germanium (Ge) has recently aroused renewed interest in microelectronics owing to its higher hole and electron mobilities as compared to silicon (Si) [1], while its high absorption coefficient in optical communication bands makes it a good candidate for the development of Ge optical devices [2].

One of the most serious issues in the fabrication of Ge devices concerns the passivation of Ge surfaces. Differently from Si, Ge forms unstable oxides: GeO_2 is water-soluble and decomposes under thermal treatment around 420 °C [3] so that it cannot be used in wet processes and thermal treatments in ULSI fabrication processes [4]. For this reason, alternative passivation coatings have been studied and developed and several Ge-based dielectric compounds (such as Ge nitrides and oxynitrides) are now considered potentially interesting for technological applications. In particular, germanium nitride (Ge_3N_4) exhibits a high dielectric constant, is water-insoluble and its thermal decomposition temperature is higher than GeO_2 [5,6] so that it could be applied not only as a buffer layer for high-k dielectrics grown on Ge substrates but also for the passivation of Ge surfaces. Germanium oxynitrides (GeO_xN_y) are also promising materials, because nitrogen incorporation in GeO_2 has proven to improve its chemical and thermal stability [7]: the decomposition temperature of a GeO_xN_y layer was found to increase up to 550 °C, which was more than 100 °C higher than that of pure GeO_2 [8,9].

A key role to tailor the passivating properties of this class of materials is played by the deposition technique. Germanium nitride and oxynitride layers are usually grown by techniques such as thermal and plasma nitridation of Ge surfaces [4,3,10], chemical vapor deposition [11] and thermal ammonolysis of GeO_2 [12,13]. Reactive sputtering technique, using N_2, NH_3 or N_2H_4 as reactive gas, has been also exploited for the deposition of germanium nitride layers [14–18]. These techniques usually require heating the substrate up to some hundreds of Celsius degrees during the film growth in order

* Corresponding author at: Dipartimento di Fisica e Astronomia G. Galilei, Università di Padova, Via Marzolo 8, I-35131 Padova, Italy.
E-mail address: maggioni@lnl.infn.it (G. Maggioni).

http://dx.doi.org/10.1016/j.apsusc.2016.10.006
0169-4332/

Table 1
Deposition parameters of germanium nitride and oxynitride films. Ge deposition rate and film composition were determined by RBS. The errors on the N and O values are around 5%.

Sample	Target-substrate distance (cm)	RF power (W)	Sample DC Bias (V)	Gas composition	Gas flow (sccm)	Ultimate pressure (Pa)	Water vapor bombardment rate (10^{13} molecules cm^{-2} s^{-1})	Ge deposition rate (10^{13} atoms cm^{-2} s^{-1})	Film composition
A	14	40	–	N_2	40	8.5×10^{-5}	3.1	10.7	$Ge_2O_{1.0}N_{2.1}$
B	5	60	–	N_2	40	4.1×10^{-5}	1.5	104	$Ge_3N_{4.6}$
C	5	60	–	N_2:Ar	25:15	3.4×10^{-5}	1.2	184	$Ge_3N_{4.0}$
D	14	40	–	N_2:Ar	20:20	8.6×10^{-5}	3.1	15.8	$Ge_2O_{1.2}N_{1.9}$
E	5	60	–	N_2:Ar	20:20	3.3×10^{-5}	1.2	171	$Ge_3N_{4.1}$
F	5	60	–	N_2:Ar	15:25	3.4×10^{-5}	1.2	197	$Ge_3N_{4.1}$
G	5	60	−20	N_2	40	1.1×10^{-4}	4.0	104	$Ge_3N_{4.6}$
H	5	60	−40	N_2	40	3.8×10^{-4}	13.7	103	$Ge_3N_{4.2}$
I	5	60	−60	N_2	40	1.1×10^{-4}	4.0	103	$Ge_3N_{4.1}$
J	5	60	−80	N_2	40	1.4×10^{-4}	5.1	93	$Ge_3N_{4.1}$
K	5	60	−100	N_2	40	1.9×10^{-4}	6.8	88	$Ge_3N_{3.7}$

to promote the reaction between germanium and nitrogen/oxygen species. This requirement can be a drawback for those applications, where the substrate can be damaged by an excessively high temperature. This is the case when the germanium (oxy)nitride coating has to be applied as a passivation layer to the intrinsic surface of a high-purity Ge (HPGe) detector [19–21]. In fact, an excessive heating can promote the unwanted diffusion of contaminant species and of Li atoms (used for the n^+ contact of Ge detectors) then jeopardizing the detector performance.

Aiming at this specific application, in this work we optimized the room temperature (R.T.) deposition of germanium nitride and oxynitride films by means of reactive RF magnetron sputtering as a technique for producing passivation coatings for Ge-based devices.

Several films were prepared under different deposition parameters, such as atmosphere composition and deposition rate, and their main physical properties were characterized. One set of films was obtained by RF biasing the substrates, in order to study the effects of the ion bombardment on the film properties.

As a final step of our study, a germanium nitride coating was deposited onto the intrinsic surface of a planar HPGe diode and the reverse leakage current of the biased diode, with and without coating, was measured and compared.

2. Experimental details

The experimental equipment used for the coatings deposition consisted of a stainless steel vacuum chamber evacuated by a turbomolecular pump to a base pressure lower than 5×10^{-4} Pa. The glow discharge sustaining device was a 2-in. cylindrical magnetron sputtering source connected to a radio frequency power generator (600 W, 13.56 MHz), through a matching box. All films were deposited at two values of the RF power: 40 W and 60 W. Pure Ge (99.999%) was used as a target. Several N_2-Ar gas mixtures were used for the depositions (see Table 1) by regulating the gas flow of each gas. The different substrates (silicon, carbon and sapphire) were placed on a sample holder at distances of 5 cm and 14 cm.

A set of films was prepared by biasing the samples with a second RF power generator (600 W, 13.56 MHz), which resulted in an average dc voltage acquired by the samples and purposely fixed at values ranging from 0 V to −100 V, in step of −20 V. In this way, a controlled ion-bombardment-assisted deposition was achieved at a constant average ion energy. The time for each deposition run was varied in order to achieve a film thickness between 100 and 300 nm. For Raman spectroscopy measurements, the deposition times were extended in order to get 600 nm thick samples. A mass spectrometer (Prisma Plus QMG 220, Pfeiffer Vacuum) revealed water vapor as the main residual component in the deposition chamber.

Rutherford Backscattering Spectrometry (RBS) was performed using 2.0 MeV $^4He^+$ beam at the Van de Graaf accelerator at the Laboratori Nazionali di Legnaro, at the scattering angle of 160°, in order to determine film deposition rate and composition. Samples were characterized by means of glancing x-ray diffraction (XRD) using a Philips diffractometer equipped with glancing-incidence X-ray optics. The analyses were performed at 0.5° incidence using CuK_α Ni filtered radiation at 40 kV and 40 mA.

The vibrational dynamics of germanium nitride samples was probed by either FT-IR or Raman spectroscopy measurements. The transmittance spectra of the samples were recorded in the 4000–400 cm^{-1} range, using a spectrometer Jasco (model FTIR 660 Plus) with a resolution of 4 cm^{-1}. Micro-Raman spectra were carried out in backscattering geometry, at room temperature, under excitation at 514.5 nm or, alternatively, at 647.1 nm by means of a triple-axis monochromator (Horiba-Jobin Yvon, model T64000), set in double-subtractive/single configuration, and equipped with holographic gratings having 1800 lines/mm. The scattered radiation was detected by a charge coupled device detector, with 1024×256 pixels, cooled by liquid nitrogen, and the spectral resolution was better than 0.6 cm^{-1}/pixel. All the spectra were calibrated in frequency using the emission lines of an Ar spectral lamp.

The surface morphology of the samples was investigated either by a SEM (Tescan Vega3 XM) equipped with the energy dispersive spectrometry (EDS) option or by a no-contact-mode AFM model C-21 (Danish Micro Engineering), mounting a DualScope Probe Scanner 95-50.

Electrical resistivity, $\rho(T)$, of films deposited on sapphire substrates was measured in a co-planar configuration as a function of the temperature from about 300 K–600 K, by using a small furnace operating in vacuum ($P < 10^{-3}$ Pa) and at dark. Four Au electrodes, about 5 mm apart, were sputtered on the film surface, near its borders. Due to the extremely high resistance exhibited by all the films, the measurements were carried out in a two contacts geometry, by using electrometers (Keithley either mod. 617 or 6517 B) operating in the V/I mode. During this work the experimental setup was updated in order to measure higher values of the sample resistance. Depending on the room temperature resistance, the applied bias ranged from 10 V to 100 V, with a typical value of 50 V. Thermal energy in the film was changed very slowly, with a rate of about 0.5–1 K/min and $\rho(T)$ collected after T stabilization to better than 1 K (typically 0.5 K). Each $\rho(T)$ value was obtained averaging 25–30 data points, collected at a fixed T value. Film resistivity was measured continuously, from room temperature (R.T.) up to 600 K and then back to R.T.

A planar, cylindrical HPGe diode of 19 mm (height) × 39 mm (diameter) was prepared in our laboratory to check the passivation properties of germanium nitride coatings. The p^+ contact was

obtained by Boron implantation over one of the planar faces of the cylinder and the n^+ contact by Li diffusion on the opposite side. Further details about diode preparation can be found in [22]. For the measurement of the leakage current, the diode without the Ge_3N_x coating was passivated by the standard methanol passivation, consisting in an etching in a 3:1 HF 40%: HNO_3 65% solution (reagent grade, Carlo Erba) for 3 min, followed by direct quenching in methanol (Erbatron, Carlo Erba). Immediately after this treatment, the diode was placed in a commercial standard cryostat, pumped down to a pressure lower than 10^{-3} Pa and cooled to about 85 K. Afterwards, the leakage current was tested by a Keithley 237 source-measurement unit (current sensitivity $\approx 10^{-14}$ A) reverse-biasing the diode at increasing voltage, with steps of 5 V every 60 s and a measurement every 5 s, until a drift of the current was observed. In order to minimize the effects of parasitic currents and capacities on the measured current, triaxial cables were used to connect the unit to the diode. It has to be pointed out that the forward bias region was not investigated, since the bulk contribution to the current obscures the surface current in this region. For the test of the coated diode, a thin Ge_3N_x layer was deposited with the same parameters of sample C (see Table 1) on the lateral surface of the same diode, by using a rotating sample holder after careful masking of the two circular faces. Immediately after the deposition, the diode was placed inside the cryostat, pumped down and cooled for the measurement. For both configurations no hysteresis effect was found.

3. Results and discussion

3.1. Film composition and structure

The experimental parameters used for the deposition of germanium nitride and oxynitride samples are reported in Table 1, together with the film deposition rates and compositions, as derived by RBS. Samples from A to F were deposited without biasing the sample holder, while for samples from G to K the average dc bias was increased from −20 V to −100 V. Data reported in Table 1 evidence how the deposition rate affects the film composition, independently of the atmosphere composition. In fact, when the deposition rate is low (samples A and D), the O/Ge atomic ratio ranges from 0.5 to 0.6 and the O/N ratio ranges from 0.45 to 0.60, while the N/Ge ratio is between 0.97 and 1.05. On the other hand, when the deposition rate is high (samples B, C and from E to K), the oxygen content drastically decreases below the detection threshold and the nitrogen content increases (N/Ge ranges from 1.21 to 1.53). Since the oxygen incorporated into the films comes mainly from the residual gases desorbed from the deposition chamber walls, the difference in the oxygen content can be ascribed to the large difference in the ratio between the deposition rate of Ge atoms, r_{Ge}, and that of oxygen-containing species on the substrate surface. Taking into account that the main component of the residual atmosphere is water vapor, as revealed by mass spectrometry measurements (see Experimental section), the bombardment rate of oxygen-containing species onto the substrate surface can be approximated to that of water vapor, r_{H2O} (Table 1). r_{H2O} was calculated from the residual pressure of water vapor immediately before the film deposition [23]. For samples A and D, the ratio between the deposition rate of Ge atoms and the bombardment rate of water vapor molecules, r_{Ge}/r_{H2O}, is less than five Ge atoms for every water vapor molecule, while for samples B, C, E and F r_{Ge}/r_{H2O} increases up to more than sixty and it is easily envisaged that it can be further enhanced by both increasing the Ge deposition rate and decreasing the ultimate pressure.

Film composition is also strongly affected by the atmosphere composition, as expected. When pure N_2 is used (sample B), the film is over-stoichiometric in nitrogen (N/Ge = 1.53 instead of 1.33). In contrast, with N_2 dilution in Ar (samples C, E and F), a stoichiometric ratio (within the experimental error) will result, in agreement with data of Lewin et al. [18].

The composition of samples from G to K evidences the effects of ion bombardment during the film growth. Firstly, the oxygen content is below the RBS detection threshold for all the biases ranging from −20 V to −100 V. This finding shows the prevailing effect of the ion bombardment on the incorporation of contaminant species in the film with respect to the residual pressure of water vapor immediately before the deposition: in fact, even if the ratio r_{Ge}/r_{H2O} in the biased samples is intermediate between the two previous sets of unbiased samples (ranging from 7.6 to 26, see Table 1), the oxygen content is still below the detection threshold. Ion bombardment of the growing layer promotes the release of weakly bonded, physisorbed water molecules from the film surface, thus holding down the oxygen incorporation. A second important effect is the trend of Ge deposition rate at increasing bias: it keeps constant until a bias of −60 V and decreases down to about 85% at −100 V. This trend shows that the Ge re-sputtering from the growing film is negligible until −60 V and becomes important starting from −80 V. The last important finding concerns the N/Ge atomic ratio, which decreases at increasing bias: the film is over-stoichiometric in nitrogen, at biases lower (less negative) than −60 V, approaches the stoichiometry (within the experimental error) at −60 V and −80 V and then drops to a substoichiometric value at −100 V. Taking into account the trend of r_{Ge}, this behavior indicates that N resputtering becomes important at lower bias values than for Ge resputtering and keeps more pronounced even at the higher bias (preferred N resputtering). All these findings evidence the straightforward way to finely control the film composition allowed by the specific deposition technique used in our study.

Concerning the structure of deposited films, XRD shows that all the films are very poorly crystallized (Fig. 1) independently of the deposition parameters, with only a broad band appearing between $2\theta = 20^\circ$ and $2\theta = 45^\circ$. In this region are located some of the most intense peaks of c-Ge_3N_4 (α-phase, JCPDS 11_69, and β-phase, JCPDS 38_1374) and c-Ge_2ON_2 [24]: these are at $2\theta = 29.26^\circ$ (201), 33.41° (210) and 36.81° (211) for α-phase Ge_3N_4, $2\theta = 34.08^\circ$ (210) for β–phase Ge_3N_4 and $2\theta = 25.88^\circ$ (201), 28.74° (300), 31.06° (020), 33.77° (301) and 36.69 (220) for c-Ge_2ON_2. In the spectra of GeO_xN_y samples (A and D) a weak signal is also found close to $2\theta = 10^\circ$, which could be ascribed to a c-Ge_2ON_2 peak ($2\theta = 9.49^\circ$ (100)) [24]. No other feature can be identified. In the case of biased samples, we can observe a clear evolution in the band shape at increasing bias (Fig. 1): the relative height of the peak placed around $2\theta = 37^\circ$ decreases with respect to the left part of the band. This trend does not seem to be due to a phase transformation but rather to a rearrangement of the nanocrystallites present in the films, whose growth orientation becomes more random, then resulting in an overall more disordered structure at increasing bias.

FT-IR analysis points out a significant difference in the spectra of films deposited at different deposition rate (Fig. 2): a single broad peak is found in the range 680 to 720 cm^{-1} for the high-deposition rate samples (B, C and from E to K), while for the low-rate ones (A and D) the peak appears around 770 cm^{-1}. Although peaks of β-phase of c-Ge_3N_4 are found at 780 and 910 cm^{-1} and α-phase of c-Ge_3N_4 has one peak at 730 cm^{-1} [25], a-Ge_3N_x samples usually exhibit a peak centered at about 700 cm^{-1}, which is assigned to Ge-N in-plane asymmetric stretching vibration [26]. This is the case for the high-rate germanium nitride samples. On the other hand, IR features of low-rate samples are clearly affected by the presence of oxygen: the absorption peak around 770 cm^{-1} is assigned to the stretching mode of the O-Ge-N group. Although the exact position of this peak in crystalline stoichiometric Ge_2ON_2 samples is found at 800 cm^{-1} [10], the peak shift to lower wavenumbers is thought to

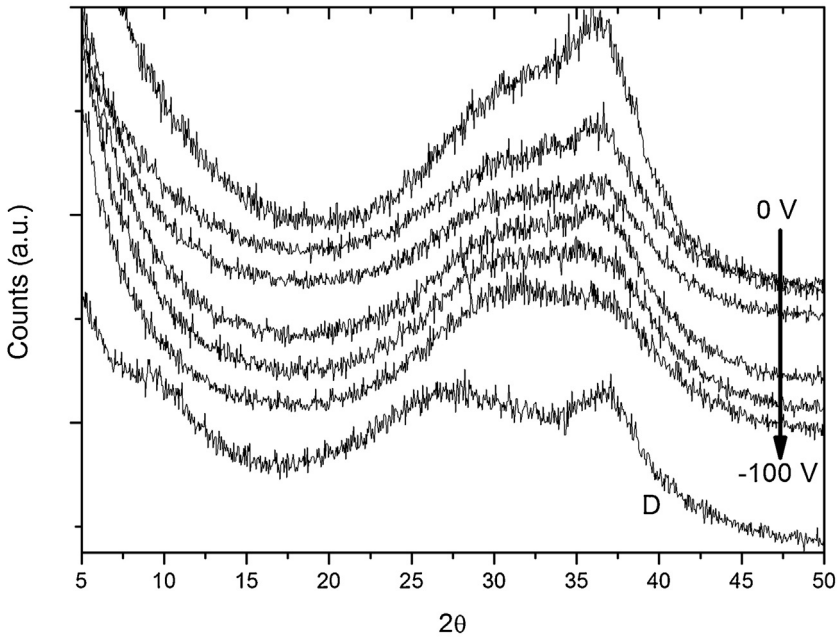

Fig. 1. XRD spectra of biased Ge_3N_x samples (B and from G to K). For comparison the spectrum of one of the two GeO_xN_y films (D) has been plotted as well. The other GeO_xN_y layer (A) shows a similar spectrum.

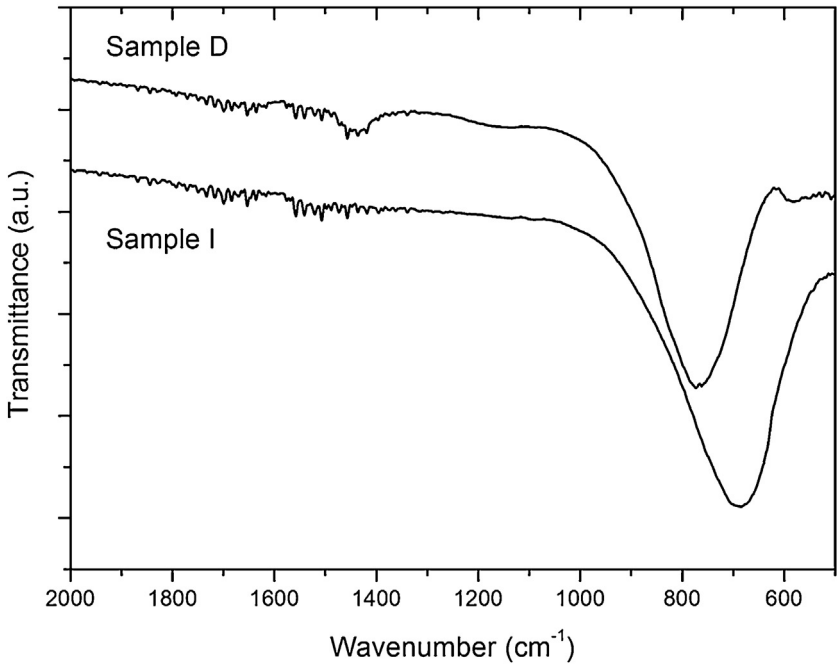

Fig. 2. FT-IR spectra of sample I (−60 V) and D (N_2:Ar 20:20, low deposition rate).

arise from the very poorly crystalline nature of these films, similarly to the germanium nitride samples.

The almost amorphous structure of germanium nitride and oxynitride films is confirmed by Raman scattering measurements. As an example Fig. 3 reports a typical Raman spectrum carried out under excitation at 647.1 nm from the highly non-stoichiometric sample B. Raman spectra of all the samples show in the low-wavenumber region a paramount, broad and asymmetric band (see in Fig. 3 the characteristic profile peaked at about 100 cm^{-1}), which is typical of systems without a long-range order, especially of glasses [27], and is related to a density of acoustic vibrational states of the system, usually referred also as the "boson peak" (BP) [28]. In addition, the same figure displays another broad spectral feature, centered at about 290 cm^{-1}, appearing in the form of a very weak shoulder of the BP, and therefore hardly observable, which is related to the translational disorder of the sample.

The Arrhenius plots of the electrical resistivity $\rho(T)$ of the different films deposited on sapphire substrates carried out in the temperature range between 300 K and 600 K are reported in Fig. 4.

The curves of films C, G and H do not exhibit values at T lower than ≈490 K, ≈450 K and ≈420 K, respectively, since their resistivity was measured before the update of the experimental setup (see the Experimental section). It is worthwhile mentioning that all the curves shown in Fig. 4 are the cooling branches of the resistivity

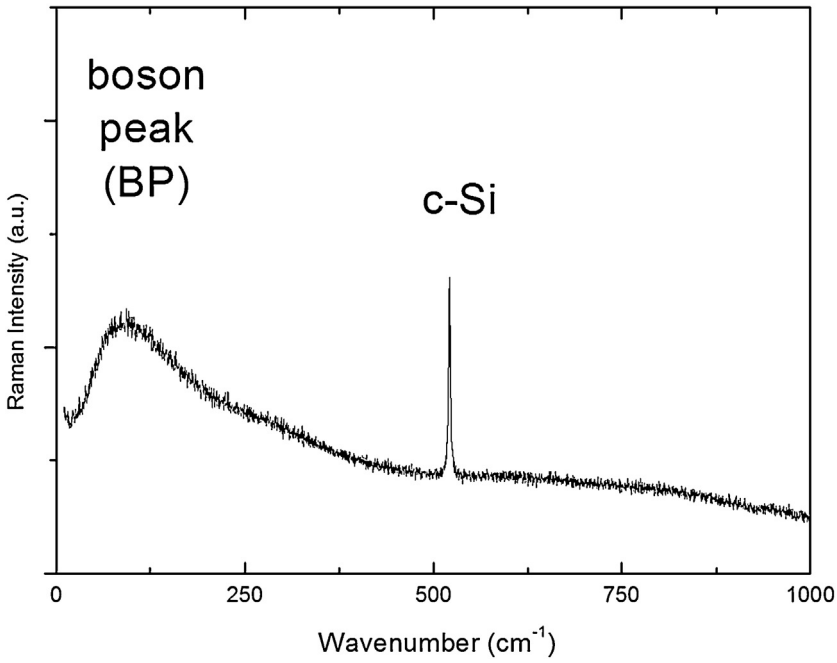

Fig. 3. Unpolarized Raman spectrum carried out under excitation at 647.1 nm from sample B. The sharp peak observed at 520 cm^{-1} is due to c-Si substrate.

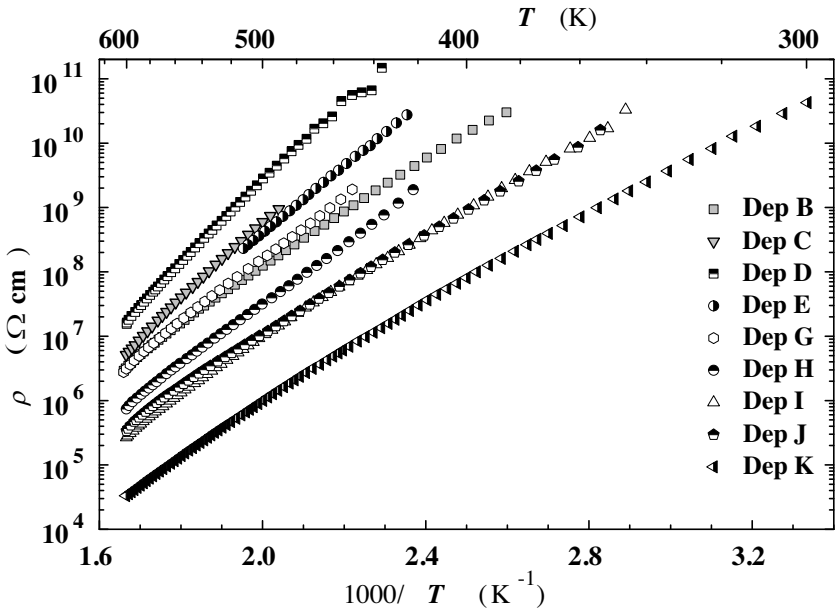

Fig. 4. Arrhenius plots of the resistivity measured, during the cooling run, for the Ge_3N_x and GeO_xN_y films (see Table 1). All the experimental data points are plotted at $\rho \leq 10^{11}\ \Omega$ cm, this value being the sensitivity limit of the measuring setup. Films C, G and H have been characterized before the update of the measuring setup (see Experimental).

measurements, because we found that, during the first cycle, the resistivity measured during the heating assumed values always lower than those measured in the cooling run. This behavior has been explained as a reduction of insulating properties of films as a consequence of their exposure to the ambient air [26,29]. This effect disappeared repeating the measurement under the same condition, keeping the sample in vacuum between two measurement runs.

The electrical resistivity measurements reveal that all the investigated films are highly insulating around R.T. (Fig. 4). In detail, apart from sample K, which is the least resistive one among those measured, all the others show a saturation in the resistance value in a T range extending from R.T. up to about 350 K ÷ 450 K, depending on the film. The resistance value detected in this T range results comparable to the insulation resistance of the measuring apparatus ($\approx 5 \times 10^{15}\ \Omega$ at 100 V of applied bias) thus suggesting that the real resistance of the films could be even higher. This implies that the resistivity of these layers is unknown around R.T.

The temperature dependence of the resistivity of all the samples is the typical one of insulating materials and it changes from about three to six orders of magnitude (Fig. 4). Moreover, the Arrhenius plots of layers resistivity exhibit some interesting features, like: i) the $\rho(T)$ curves of the biased Ge_3N_x samples (B and from G to K) show a downward shift at bias values lower than −20 V. This is essentially related to two concomitant effects: the corresponding

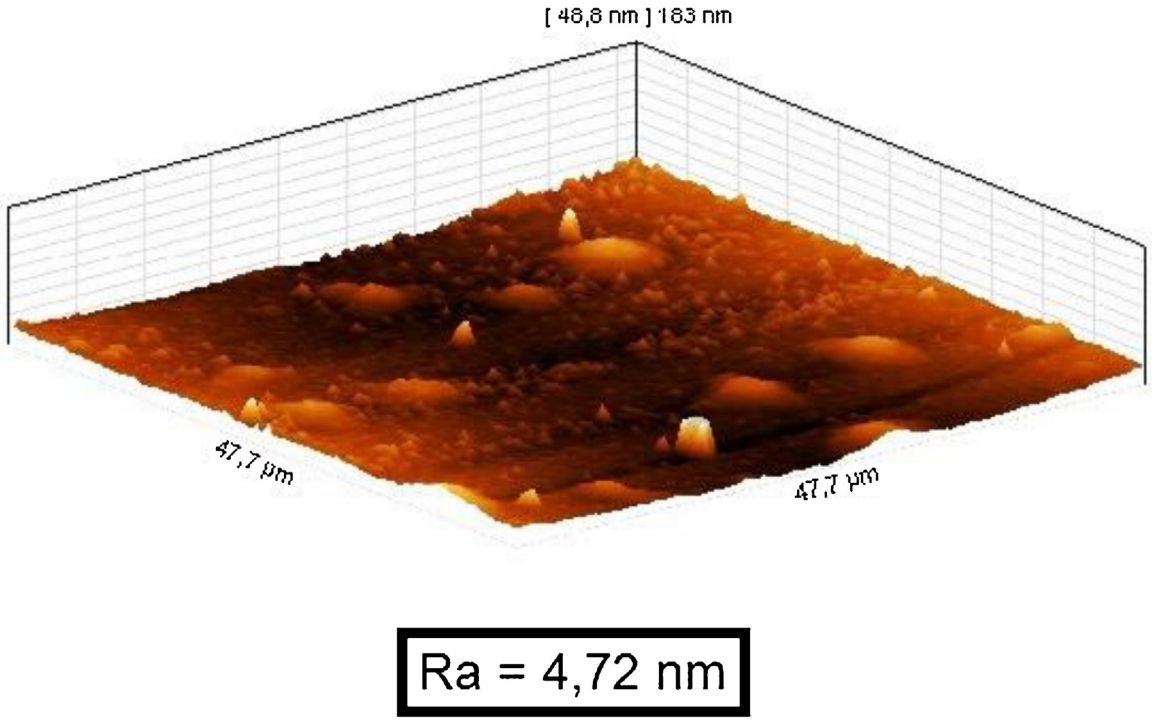

Fig. 5. AFM image of the surface of sample B.

lowering of N/Ge atomic ratio in the film, as already found by other authors in the case of understoichiometric Ge_3N_x films ($x \leq 1.6$) [26][26 and refs. therein] and the increase of disorder induced by the ion bombardment, as shown by XRD and FT-IR results, which gives rise to a more defective structure with a higher number of localized states in the band gap and then to a reduced resistivity; ii) the $\rho(T)$ curves of Ge_3N_x films deposited with the Ar + N_2 gas mixtures (i.e. films C and E) are very similar and partially overlap each other. This result demonstrates a high reproducibility of the film properties (at least from the electrical point of view) and the tight relation between resistivity and film composition. It is worthwhile noting that resistivity of these films is even higher than that of the overstoichiometric ones (B and G). iii) The $\rho(T)$ for the germanium oxynitride sample (film D) is the highest among those measured in our experiments. A comparison of our results with those in the literature for Ge_3N_x layers [26,30] shows that the resistivity of our coatings is several orders of magnitude higher, essentially due to the different N content. This also involves a change of the conduction mechanism: in the case of strongly under-stoichiometric films, the conduction is dominated by a variable range hopping mechanism [26,30], while over- and stoichiometric films show a thermally activated conduction as detailed in Ref. [31].

Analysis of the $\rho(T)$ curves reveals the existence of several activation energies, E_a, for each layer. The E_a values range from ≈0.6 eV around 350 K to ≈1.4 eV around 600 K, depending on the film [31]. Considered that the band-gap in this class of materials is expected to range from 4.5 to 5.5 eV, we deduce that the measured E_a values must be related to charge carriers transitions involving localized states inside the energy-gap, whose origin is due to the presence of defects. Due to the lacking of literature data about the nature and properties of electronic states in Ge_3N_x and GeO_xN_y, we have taken into account defect states present in the Si_3N_x system [32], which is very similar to the investigated Ge_3N_x system. Theoretical calculations and experiments demonstrate that in the Si_3N_x system a paramagnetic centre forming a π^* state is located 0.5 eV above the valence band (VB) edge [33]. Charge carrier transition from the VB edge to this π^* state can account for the lowest E_a values measured around 350 K. At higher T (≈600 K) charge carrier transitions may involve localized states farther from the VB edge, resulting in the observation of higher E_a values.

A detailed analysis of the electrical properties revealed that all the investigated Ge_3N_x and GeO_xN_y films follow the Meyer-Neldel rule [34,31].

Finally, SEM and AFM images of the as deposited films (Fig. 5) show a very homogeneous and smooth surface with a typical average roughness, R_a, below 10 nm.

3.2. Ge_3N_x-coated HPGe diode

A test to check the effectiveness of Ge_3N_x films as a surface passivation layer has been carried out, fabricating a planar HPGe diode and measuring its reverse leakage current, both with and without (see the Experimental) a Ge_3N_x film deposited onto its lateral intrinsic surface. The Ge_3N_x layer was deposited with the same parameters of sample C (see Table 1). In order to evidence only the effects of the surface passivation, the same diode was used for both measurements. In this way the results were not affected by possible differences in the bulk properties arising from the history of different diodes. The current-voltage (I–V) characteristics, measured in both the above configurations (i.e.: with and without the Ge_3N_x film) by biasing the diode up to a maximum of 80 V, are reported in Fig. 6. The reverse leakage current keeps very low (below 10 pA) up to 35 V, for both configurations, with a comparable trend. At higher voltages, the two curves part from each other and the leakage current of the uncoated device starts to exponentially increase and goes over 1 nA already at 60 V. This behaviour highlights the defective nature of this diode; in fact, if one takes into account the characteristics of this device, the drift of the leakage current should start at much higher voltages [22]. This outcome indicates that, in addition to the surface leakage current, we have to take into account a strong contribution from bulk currents, arising from defective contacts. This fact prevents us from testing the coating properties at voltages higher than 80 V. However, a positive and necessary premise for future applications is given by the behaviour

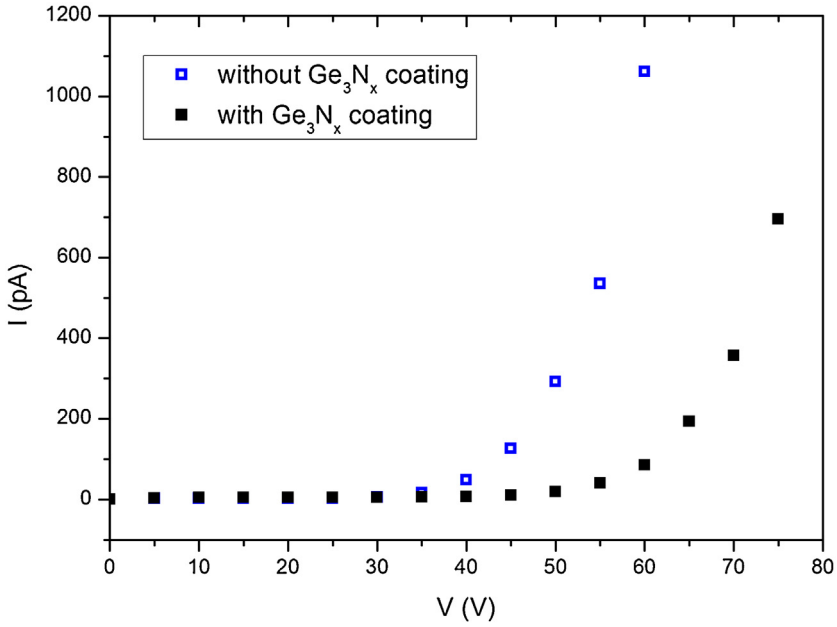

Fig. 6. I–V characteristic of a planar HPGe diode coated with Ge_3N_x film (deposited under the same nominal conditions of sample C, see Table 1) compared to that of the same diode passivated with methanol solution (see the Experimental).

of the Ge_3N_x coated diode at these low voltages. In fact, Fig. 6 shows that the leakage current starts to drift at a higher voltage than the uncoated one. At 60 V the current is around 100 pA and is still below 1 nA at 75 V. This result allows us concluding that the Ge_3N_x coating does not increase the surface leakage current, at least at voltages lower than 80 V. Taking into account that one of the contributions to the surface leakage current comes from the conduction in the passivating film, even better results could be maybe reached by using GeO_xN_y coatings, since the resistivity of these last films is much higher (see e.g. curve D in Fig. 4). It is clear that this result is only preliminary and that more complete tests on well-performing diodes and detectors are still required in order to quantitatively evaluate the improved performance of this class of materials as passivating coatings.

4. Conclusions

In view of the application to the surface passivation of germanium-based radiation detectors, we produced and investigated in detail the physical properties of germanium nitride and oxynitride films, deposited at room temperature by reactive RF magnetron sputtering. We found that the film composition was strongly affected by the deposition rate, ultimate pressure and deposition atmosphere composition. At low deposition rates germanium oxynitride films were obtained. At increasing deposition rate and decreasing ultimate pressure, the oxygen incorporation in the film drastically decreased and germanium nitride coatings were deposited. In this case, the films were over-stoichiometric in N when pure N_2 was used as deposition gas, but became stoichiometric when Ar/N_2 gas mixtures were used. The film stoichiometry was strongly affected by an applied dc substrate bias, going from over-stoichiometry in nitrogen at low biases down to under-stoichiometry at increasing bias. In biased films, the oxygen content was always below the RBS detection threshold. All the films were very poorly crystallized and resulted to be highly insulating at room temperature, their resistivity being strictly related to the film composition and deposition parameters.

The improved performance of a Ge_3N_x-coated HPGe diode was assessed by comparing the leakage current of the coated diode with that of a diode with a standard surface passivation. The promising results of this first test are an important premise for the application of these treatments as passivation routes of HPGe detectors, wherein an extremely low leakage current is of fundamental importance to assure a good energy resolution in the detection of gamma radiation. Further and exhaustive tests are going to be carried out to identify the best performing coatings and then attain their complete and quantitative validation.

Acknowledgements

The research leading to these results received funding from the Third Scientific Commission of the Istituto Nazionale di Fisica Nucleare and from the European Union Seventh Framework Programme FP7/2007-2013 under Grant Agreement no. 262010—ENSAR. The EC is not liable for any use that can be made on the information contained herein.

References

[1] K. Saraswat, C.O. Chui, T. Krishnamohan, D. Kim, A. Nayfeh, A. Pethe, Mater. Sci. Eng. B 135 (2006) 242.
[2] J. Liu, D.D. Cannon, K. Wada, Y. Ishikawa, S. Jongthammanurak, D.T. Danielson, J. Michel, L.C. Kimerling, Appl. Phys. Lett. 87 (2005) 011110.
[3] T. Maeda, T. Yasuda, M. Nishizawa, N. Miyata, Y. Morita, J. Appl. Phys. 100 (2006) 014101.
[4] K. Kato, H. Kondo, M. Sakashita, S. Zaima, Thin Solid Films 518 (2010) S226.
[5] T. Maeda, T. Yasuda, M. Nishizawa, N. Miyata, Y. Morita, Appl. Phys. Lett. 85 (2004) 3181.
[6] K. Prabhakaran, T. Ogino, Surf. Sci. Lett. 387 (1997) L1068.
[7] C.O. Chui, F. Ito, K.C. Saraswat, IEEE Electron. Dev. Lett. 25 (2004) 613.
[8] K. Kutsuki, I. Hideshima, G. Okamoto, T. Hosoi, T. Shimura, H. Watanabe, Jpn. J. Appl. Phys. 50 (2011) 010106.
[9] D. Kuzum, Interface-Engineered Ge MOSFETs for Future High Performance CMOS Applications, Stanford University, 2009, PhD Thesis.
[10] D.J. Hymes, J.J. Rosenberg, J. Electrochem. Soc. 135 (1988) 961–965.
[11] D.M. Hoffman, S.P. Rangarajan, S.D. Athavale, D.J. Economou, J. Liu, Z. Zheng, W. Chu, J. Vac. Sci. Technol. A 13 (1995) 820.
[12] C. Tindall, J.C. Hemminger, Surf. Sci. 330 (1995) 67.
[13] K. Maeda, N. Saito, Y. Inoue, K. Domen, Chem. Mater. 19 (2007) 4092.
[14] I. Chambouleyron, Appl. Phys. Lett. 47 (1985) 117.
[15] F. Boscherini, A. Filipponi, S. Pascarelli, F. Evangelisti, S. Mobilio, F.C. Marques, I. Chambouleyron, Phys. Rev. B 39 (1989) 8364.
[16] H. Yokomichi, T. Okina, M. Kondo, Y. Toyoshima, J. Non-Cryst. Solids 198–200 (1996) 379.

[17] S. Kikkawa, H. Morisaka, Solid State Commun. 112 (1999) 513.
[18] E. Lewin, M. Parlinska-Wojtan, J. Patscheider, J. Mater. Chem. 22 (2012) 16761.
[19] E.L. Hull, R.H. Pehl, J.R. Lathrop, B.E. Suttle, Nucl. Instrum. Methods Phys. Res. A 626–627 (2011) 39.
[20] R.D. Baertsch, R.N. Hall, IEEE Trans. Nucl. Sci. 17 (1970) 235.
[21] R.H. Pehl, R.C. Cordi, F.S. Goulding, IEEE Trans. Nucl. Sci. 19 (1972) 265.
[22] G. Maggioni, D.R. Napoli, J. Eberth, M. Gelain, S. Carturan, M.G. Grimaldi, S. Tatì, Eur. Phys. J. A 51 (2015) 141.
[23] B.N. Chapman, Glow Discharge Processes: Sputtering and Plasma Etching, Wiley, 1980.
[24] J.D. Jorgensen, S.R. Srinivasa, J.C. Labbe, G. Roult, Acta Crystallogr. B 35 (1979) 141–142.
[25] L. Chunrong, X. Jingzhou, X. Zheng, Vacuum 42 (1991) 1061.
[26] I. Chambouleyron, A. Zanatta, J. Appl. Phys. 84 (1998) 1.
[27] G. Carini, M. Cutroni, A. Fontana, G. Mariotto, F. Rocca, Phys. Rev. B 29 (1984) 3567.
[28] S. Ciliberti, T.S. Grigera, V. Martín-Mayor, G. Parisi, P. Verrocchio, Nature 422 (2003) 289.
[29] W. Paul, S.J. Jones, W.A. Turner, Philos. Mag. B 63 (1991) 247.
[30] I. Honma, H. Kawai, H. Komiyama, K. Tanaka, J. Appl. Phys. 65 (1989) 1074.
[31] N. Pinto, F. Caproli, G. Maggioni, S. Carturan, D.R. Napoli, J. Non-Crystalline Solids 452 (2016) 280.
[32] S.S. Makler, G. Martins da Rocha, E.V. Anda, Phys. Rev. B 41 (1989) 5857.
[33] J. Robertson, Philos. Mag. B 69 (1994) 307.
[34] W. Meyer, H. Neldel, Zh. Tekh Fiz. 12 (1937) 588.